ENVIRONMENTAL ENGINEERING SCIENCE
Volume 21, Number 6, 2004

Effect of Acidity and Elevated P_{CO_2} on Acid Neutralization within Pulsed Limestone Bed Reactors Receiving Coal Mine Drainage

Barnaby J. Watten,[1,*] Philip L. Sibrell,[1] and Michael F. Schwartz[2]

[1]United States Geological Survey
Leetown Science Center
Kearneysville, WV 25430
[2]The Conservation Fund's Freshwater Institute
Shepherdstown, WV 25443

ABSTRACT

Limestone has potential for reducing reagent costs and sludge volume associated with the treatment of acid mine drainage (AMD), but its use has been restricted by slow dissolution rates and sensitivity to scale forming reactions that retard transport of H^+ at the solid–liquid interface. We evaluated a pulsed limestone bed (PLB) remediation process designed to circumvent these problems through use of intermittently fluidized beds of granular limestone and elevated carbon dioxide pressure. PLB limestone dissolution (LD, mg/L), and effluent alkalinity (Alk, mg/L) were correlated with reactor pressure (P_{CO_2}, kPa), influent acidity (Acy, mg/L) and reactor bed height (H, cm) using a prototype capable of processing 10 L/min. The PLB process effectively neutralized sulfuric acid acidity over the range of 6–1033 mg/L (as $CaCO_3$) while generating high concentrations of alkalinity (36–1086 mg/L) despite a hydraulic residence time of just 4.2–5.0 min. Alk and LD (mg/L $CaCO_3$) rose with increases in influent acidity and P_{CO_2} ($p < 0.001$) according to the models: $Alk = 58 + 38.4\ (P_{CO_2})^{0.5} + 0.080\ (Acy) - 0.0059(P_{CO_2})^{0.5}\ (Acy)$; $LD = 55 + 38.3\ (P_{CO_2})^{0.5} + 1.08\ (Acy) - 0.0059\ (P_{CO_2})^{0.5}\ (Acy)$. Alkalinity decreased at an increasing rate with reductions in H over the range of 27.3–77.5 cm ($p < 0.001$). Carbon dioxide requirements ($Q(avg)_{CO_2}$, L/min) increased with P_{CO_2} ($p < 0.001$) following the model $Q(avg)_{CO_2} = 0.858\ (P_{CO_2})^{0.620}$, resulting in a greater degree of pH buffering (depression) within the reactors, a rise in limestone solubility and an increase in limestone dissolution related to carbonic acid attack. Corresponding elevated concentrations of effluent alkalinity allow for sidestream treatment with blending. Numerical modeling demonstrated that carbon dioxide requirements are reduced as influent acidity rises and when carbon dioxide is recovered from system effluent and recycled. Field trials demonstrated that the PLB process is capable of raising the pH of AMD above that required for hydrolysis and precipitation of Fe^{3+} and Al^{3+} but not Fe^{2+} and Mn^{2+}.

Key words: acid mine drainage; limestone dissolution; carbon dioxide; acidity; bed height; dissolved metals; pulsed bed reactors; treatment; alkalinity; pressure

*Corresponding author: U.S. Dept of the Interior, U.S. Geology Survey, Leetown Science Center, 11649 Leetown Road, Kearneysville, WV 24530. *Phone:* 304-724-4425; *Fax:* 304-724-4428; *E-mail:* barnaby_watten@usgs.gov

INTRODUCTION

Acidic mine drainage (AMD) is a major source of pollution in surface waters within the coal deposit regions of many parts of the world including Appalachia (CEQ, 1981; Maree *et al*., 1996). AMD often renders receiving waters unfit for domestic use and unable to support desirable plant or animal communities (Starnes and Gasper, 1995; Cole *et al*., 2001a, 2001b). AMD is produced by oxidation of metallic sulfides, primarily FeS_2, present with coal in mines or refuse piles (Evangelou, 1995):

$$FeS_2 + 3.5\ O_2 + H_2O \rightarrow Fe^{2+} + 2\ SO_4^{2-} + 2\ H^+ \quad (1)$$

$$Fe^{2+} + 0.25\ O_2 + H^+ \rightarrow Fe^{3+} + 0.5\ H_2O \quad (2)$$

Oxidation is followed by a hydrolysis reaction that generates an insoluble oxyhydroxide product:

$$Fe^{3+} + 3\ H_2O \rightarrow Fe(OH)_3 + 3\ H^+ \quad (3)$$

Acidification provides for solubilization of certain base metals, including Al^{3+} and Mn^{2+}, that contribute acidity while undergoing secondary hydrolysis reactions (Evangelou, 1995):

$$Al^{3+} + 3\ H_2O \rightarrow Al\ (OH)_3 + 3\ H^+ \quad (4)$$

$$Mn^{2+} + 0.25\ O_2 + 1.5\ H_2O \rightarrow MnOOH + 2\ H^+ \quad (5)$$

Treatment of AMD is typically achieved through direct addition of alkaline material followed by gravity separation of insoluble reaction products. Alkaline materials used include anhydrous ammonia, sodium hydroxide, calcium oxide, and limestone (Skousen, 1998). Limestone has potential for reducing treatment costs given that its market value, on an equivalent or acid neutralization basis, is a fraction (0.03 to 0.26) of the alternative reagents (Hedin *et al*., 1994). Its use also reduces sludge volume (Dempsey and Jeon, 2001; Sibrell and Watten, 2003) and risk of over treatment (Olem, 1991) while providing calcium ions needed to moderate toxicity of certain dissolved metals (Wilmoth, 1974; Ingersoll *et al*., 1990). These benefits are offset, however, by limestone's relatively slow dissolution rate and sensitivity to passivation or armoring by certain scale forming reactions that inhibit transport of H^+ and its products at the solid–liquid interface (Lovell, 1973; Ziemkiewicz *et al*., 1997). Scales of particular concern include Fe, Al, and Mn oxides as well as gypsum ($CaSO_4 \cdot 2H_2O$) (Lovell, 1973; Pearson and McDonnell, 1975a; Sverdrup, 1984).

Dissolution rates of limestone impaired by scale have been diminished by a factor of 5 (Pearson and McDonnell, 1975b) reducing application to those sites that (1) can accommodate unusually long hydraulic retention times or (2), allow use of equipment designed to grind and abrade crushed limestone surfaces. The latter includes water powered tumbling drums (Zurbuch, 1963) and electric powered autogenous mills (Lovell, 1973). More recently (Sverdrup, 1984; Maree and du Plessis, 1994), fluidized bed technology has been adapted from early industrial applications (Ghem, 1944; Eden and Truesdale, 1950; Wheatland and Borne, 1962) so as to eliminate the need for high-torque drive components and associated power requirements. Here, abrasion of the limestone surface is provided by interparticle collision forces generated hydraulically during bed expansion. Fluidized bed designs have been based primarily on the reversible first-order reaction of calcite, and its products, with hydrogen ions (Maree and du Plessis, 1994; Maree *et al*., 1996):

$$CaCO_3 + H^+ \rightarrow HCO_3^- + Ca^{2+} \quad (6)$$

$$HCO_3^- + H^+ \rightarrow H_2CO_3 \rightarrow H_2O + CO_2 \quad (7)$$

Plummer *et al*. (1978) identified two additional dissolution reactions that can occur simultaneously:

$$CaCO_3 + CO_2 + H_2O \rightarrow Ca^{2+} + 2\ HCO_3^- \quad (8)$$

$$CaCO_3 + H_2O \rightarrow Ca^{2+} + HCO_3^- + OH^- \quad (9)$$

Combining Equations (6), (8), and (9), Sverdrup (1984) developed an overall kinetic expression for calcite particles >10 microns:

$$-\frac{dm}{dt} = [k_1[H^+] + k_2[CO_2] + k_w - k_b([Ca^{++}][HCO_3^-])] \cdot \left(\frac{3m}{\rho r}\right) \quad (10)$$

where [ ] refers to the bulk solution concentration, k_1 and k_2 are first order reaction constants, k_w is a zero-order constant for Equation (9), k_b is a constant for the backward reaction driven by the interaction of Ca^{2+} and HCO_3^- with calcite, m is mass of particle, ρ is the density of the limestone, and r is particle radius. Certain rate constants are defined by hydrodynamic conditions and temperature, for example, k_1 can be estimated with the relation (Sherwood *et al*., 1975):

$$k_1 = \frac{D}{r} \cdot (1 + 0.3Re^{1/2}Sc^{1/3}) \quad (11)$$

where D is diffusivity, and Re and Sc are the Reynold's and Schmidt numbers, respectively. Inspection of Equations (10) and (11) reveals calcite dissolution is accelerated under conditions of low pH, high free carbon dioxide concentrations (DC), high turbulence and when particle size (r) is small. However, reducing the particle size in a fluidized bed significantly lowers fluid flux rates required for bed expansion (Summerfelt and Cleasby, 1993). This response limits turbulence and interparticle collision forces (Cleasby and Baumann,

1977), resulting in excessive scaling of limestone surfaces (Ghem, 1944; Maree *et al*., 1992; Maree and du Plessis, 1994).

Watten (1999) described a pulsed limestone bed (PLB) process designed to prevent scale development at low mean flux rates. Here, a control system directed AMD intermittently into reactors to establish a repeating cycle of fluidization, bed turnover, and contraction. During bed expansion, AMD was introduced at a high rate through nozzles designed to accelerate particle attrition. Expansion was interrupted prior to carryover of the limestone bed into the reactors' effluent. Further, a carbon dioxide pretreatment step was used to accelerate limestone dissolution by forcing Equation (8) and by minimizing, temporarily, the rise in pH that occurs during treatment [Equation (7)]. High dissolved carbon dioxide levels also elevated equilibrium concentrations of HCO_3^- (Stumm and Morgan, 1996), and thereby allowed for surplus acid neutralization capacity (alkalinity) in the reactors' effluent like that observed in anoxic limestone drains (Hedin *et al*., 1994; Mitchell and Wildeman, 1996). Dissolved carbon dioxide was stripped from the reactors' effluent, and then reused to minimize makeup CO_2 requirements. Decarbonation of effluent reduced acidity, forcing a desirable upward shift in equilibrium pH (Pearson *et al*., 1982).

Field tests of the PLB process have demonstrated its ability to effectively treat AMD containing moderate and high concentrations of Fe^{3+} and Al^{3+} (Sibrell *et al*., 2000, 2003). Lee (2003) evaluated the effects of hydraulic residence time and temperature on PLB performance in the laboratory with simulated AMD. Sibrell and Watten (2003) evaluated PLB metal sludge products including relative volume, filterability, and settlability. Our objective was to correlate PLB limestone dissolution, and effluent alkalinity, with carbon dioxide feed rate, influent acidity, and reactor bed height so as to explore further the treatment potential of the process.

METHODS

We constructed an AMD neutralization system capable of processing 10 L/min. Figure 1 shows the system's major components—four 10-cm diameter × 160-cm vertical reaction columns charged with granular limestone, a 0.26-kW centrifugal pump (stainless steel) coupled with a 10-cm diameter × 160-cm packed tower carbonator and a time-based electronic control system (ChronTrol Corporation, San Diego, CA) used to direct the system's electrically activated ball valves (Hayward Industrial Products, Inc., Elizabeth, NJ). Reaction columns and the carbonator were designed as pressure vessels with transparent (PVC) walls. The carbonator was packed with 155 cm of Tellerette® type (47 × 19 mm) plastic packing with

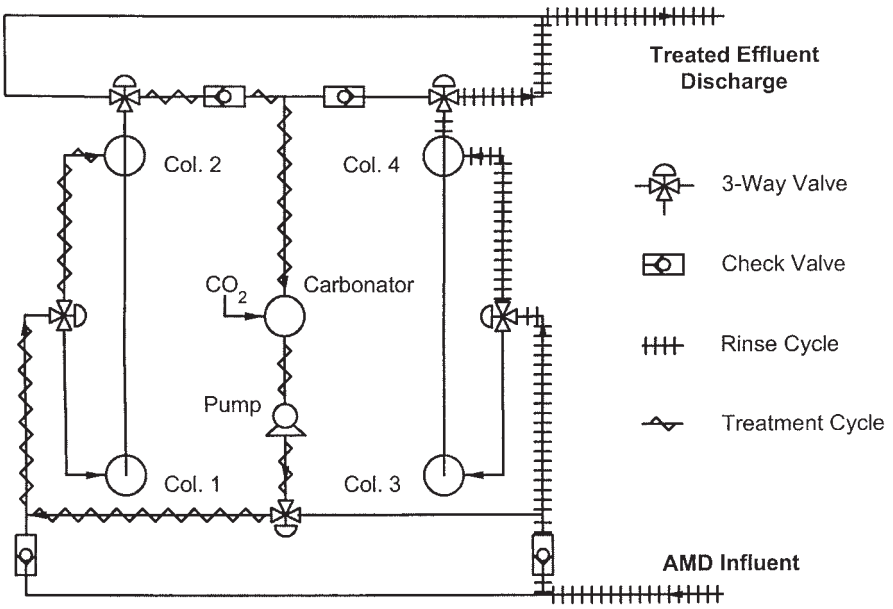

Figure 1. Plan view of the pulsed limestone bed AMD treatment system. In this example, limestone columns 1 and 2 are linked temporarily in a closed (treatment cycle) loop that includes a sealed packed tower carbonator. Within this loop recirculated AMD is directed alternately into each column at 1-min intervals. Concurrently, limestone columns 3 and 4 are receiving untreated AMD, alternately, at 1-min intervals during a temporary rinse/reloading cycle. The three-way valves shown are synchronized by a time-based control system that maintains a repeating 4-min cycle of rinse/reloading and treatment for each column pair.

a specific surface area of 185 m^2/m^3. In operation, each set of two reaction columns (1 and 2 or 3 and 4) were alternately loaded with AMD, then separated from the influent and treated with a recycled flow with a high partial pressure of CO_2, and then returned to the AMD influent line for rinse and loading. Treatment and rinse/loading phases were each fixed at 4 min. Bed expansion and contraction is achieved by directing flow intermittently (every other minute) through a 6.4-mm orifice positioned at the base of each column. Column overflow is returned to the carbonator for additional absorption of CO_2 prior to redistribution among the two columns in the closed treatment loop. Pressurization is provided by pure CO_2 entering the carbonator from a Dewar-type storage tank. Pressure is set and maintained by the tank's two-stage regulator regardless of changes in CO_2 feed requirements. At the end of each 4-min cycle columns involved in the treatment phase (e.g., columns 1 and 2, Fig. 1) are isolated from the carbonator by the control system, then coupled to the drain system allowing treated AMD to be displaced from each reactor intermittently (every other minute) by an incoming charge of untreated AMD. Concurrently, columns involved in the loading phase (e.g., columns 3 and 4, Fig. 1) are coupled with the carbonator in a second closed loop, pressurized, then alternately expanded like columns 1 and 2 so as to treat the AMD charge received during their previous 4-min cycle. Continued operation as described allows sequential (batch) loading and treatment of AMD while also providing a constant discharge. Further, a single carbonator and recycle pump is used to support treatment within both pairs of the reaction columns.

Test Series I—laboratory trials

We established effects of carbon dioxide on acid neutralization using carbonator pressures of 0, 70, 210, 410, and 690 kPa at each of four inlet acidities—about 6, 200, 560, and 1,020 mg/L. Acid solutions were prepared by mixing reagent grade sulfuric acid with well water. Water inflow and recirculation rates were fixed at 9.5 and 8.5 L/min, respectively. Cycle duration was 4 min. Reaction columns were each charged with 7.0 kg of limestone sand rinsed previously of fines with well water at a flux of 1.5 $m^3/m^2 \cdot$ min for 30 min. The limestone used (Bell Mine Glass Stone #1, Bellefonte Lime Co., Bellefonte, PA) was 96.9% $CaCO_3$, had an effective size (D_{60}) of 525 μm, and a uniformity coefficient (D_{60}/D_{10}) of 3.3. Initial use of a limestone charge was preceded by a 2.5-h run with well water at 124 kPa. Resultant settled bed heights prior to testing were 62.5–63.0 cm. Limestone was replaced when bed height fell below 56 cm. Test conditions were repeated once or twice (41 observations). Cycle duration was then increased from 4 to 8 min at three test carbonator pressures (0, 210, 690 kPa) and two inflow acidities (10 and 1,000 mg/L). Test conditions here were repeated twice. Bed height effect on acid neutralization was also established by following changes in treatment effect with time (70 observations) without limestone replacement. Operating pressure during these tests was 140 kPa. Influent acidity was about 370 mg/L. Water inflow and recirculating flow were both 8.0 L/min with initial and final bed heights of 77.5 and 27.5 cm. Carbon dioxide feed requirements were measured in a subsequent test using a similar influent acidity (350 mg/L). Operating pressures here were 5, 70, 140, and 280 kPa with water inflow and recirculating flow each set at 9.5 L/min. Carbon dioxide flow rate and corresponding treatment cycle pH were recorded during 3 or 4 consecutive 4-min cycles using an electronic data logger coupled with a mass flow meter (AALBORG®, Orangeburg, NY) and an in-line pH probe (Signet®, El Monte, CA) located on the carbonator effluent line.

Test Series II—field trials

Field tests of the PLB prototype were completed in cooperation with the PA Dept. of Environmental Protection at the Toby Creek AMD Treatment Plant, Dagus Mines, PA. AMD from Portal A, located immediately adjacent to the treatment plant, was pumped through the prototype at each of three operating pressures (70, 140, 190 kPa). A second test compared performance, without CO_2 input, when treating AMD from Portal A and a second source identified here as Kyler Run. Cycle duration in all tests was 4 min, and effluent observations were repeated once or twice.

Analytical techniques

Treatment effect in Test Series I and II was established by comparing influent with effluent chemistry. Effluent samples were composites taken at a fixed rate during a complete 4- or 8-min cycle. Test Series I analyses followed APHA (1995) and included temperature, pH, alkalinity and acidity. Limestone dissolution was calculated as the sum of acidity neutralized and alkalinity added by the treatment. Test Series II analyses were performed by the PA Dept. of Environmental Protection, Harrisburg PA. Analyses were based on EPA methods and included pH, alkalinity, hardness, Ca^{2+}, SO_4^{2-}, Fe_T (total iron), Fe^{2+}, Mn^{2+}, Al^{3+}, and acidity (hot peroxide treatment). Effluent samples were analyzed here following a 7-min air-stripping step both with and without subsequent filtering through a Whatman® 934 AH glass fiber filter (1.5-μm pore size). Influent temperature and dissolved oxygen were measured with a polarographic oxygen meter (Yellow

Springs Instrument Co., Yellow Springs, OH). Influent CO_2 tension (mm Hg) was determined with a head-space analyzer (Watten *et al*., 2003) coupled with an infrared CO_2 gas phase meter (CEA Instruments, Emerson, NJ). During all tests water flow rate was measured with a paddle wheel flow sensor (Signet®, El Monte, CA) or by measuring time required to fill a container of known volume. Local barometric pressure was measured with a pressure transducer (Solomat® Model MPM 2019). Hydraulic residence time (HRT) was calculated as the total reactor volume, minus the volume of water displaced by the limestone, divided by influent flow rate. Statistical analyses were completed using either the Statistical Analysis System (SAS®, version 8.0) or SigmaStat® (version 2.0) software. Specific analyses included Student's *t*, analysis of variance, linear regression, multiple linear regression, and the Mann-Whitney rank sum test.

RESULTS

Test series I—laboratory trials

The PLB prototype was effective in neutralizing sulfuric acid acidity over the range of conditions evaluated while concurrently providing high levels of effluent alkalinity. HRT ranged from about 4.2 to 5.0 min. In initial tests, mean inlet acidities measured at each of five operating pressures were 6.4 mg/L (range, 3.4–9.6), 200.5 mg/L (range, 199.0–200.9), 557.8 mg/L (range, 553.9–562.5), and 1,019.5 mg/L (range, 1,005.7–1,032.9). Corresponding inlet pH averaged, respectively, 6.57, 2.60, 2.22, and 2.04. Inlet temperature was, in all cases, 9.5°C. Reactor effluent temperatures averaged 10.5°C (SD, 0.28). Bed heights increased during expansion from a mean, without flow, of 60.0 cm (SD, 2.2) to a mean of 125.0 cm (SD, 2.96) with flow. Local barometric pressure averaged 736 mmHg (SD, 2.5). Figure 2 shows that the mass of limestone reacted per liter treated (LD, mg/L as $CaCO_3$) increased with inlet acidity (Acy) and operating pressure (P_{CO2}) to an unusually high value of 2,041.8 mg/L. Slopes of the plot LD vs. $(P_{CO_2})^{0.5}$ established for acidities of 6.4 and 200.5 mg/L were indistinguishable as were slopes established for the acidity pair of 557.8 and 1,019.5 mg/L ($p > 0.05$). However, slope of the plots established for the two lower acidities exceeded slopes established for the high acidity pair ($p < 0.01$). Factor effects (Acy and $P_{CO_2}{}^{0.5}$) and interactions (Acy $\cdot$ $P_{CO_2}{}^{0.5}$) on limestone dissolution were statistically significant ($p < 0.01$). The resultant linear model describing limestone dissolution is:

$$LD = 55 + 38.3 \cdot (P_{CO_2}{}^{0.5}) + 1.08 \cdot (Acy) - 0.0059 \cdot (P_{CO_2}{}^{0.5}) \cdot (Acy) \quad (12)$$

$$R^2 = 0.994;\ p < 0.0001;\ df = 37;\ F = 2183.93$$

Figure 3 gives effluent alkalinity concentrations that correspond to the limestone dissolution values modeled. Alkalinity (Alk) increased with P_{CO_2} from a low of 36.2 mg/L to a high of 1,086.2 mg/L. Again, factor effects (Acy and $P_{CO_2}{}^{0.5}$) and interactions (Acy $\cdot$ $P_{CO_2}{}^{0.5}$) were statistically significant ($p < 0.01$). The resultant linear model describing effluent alkalinity is:

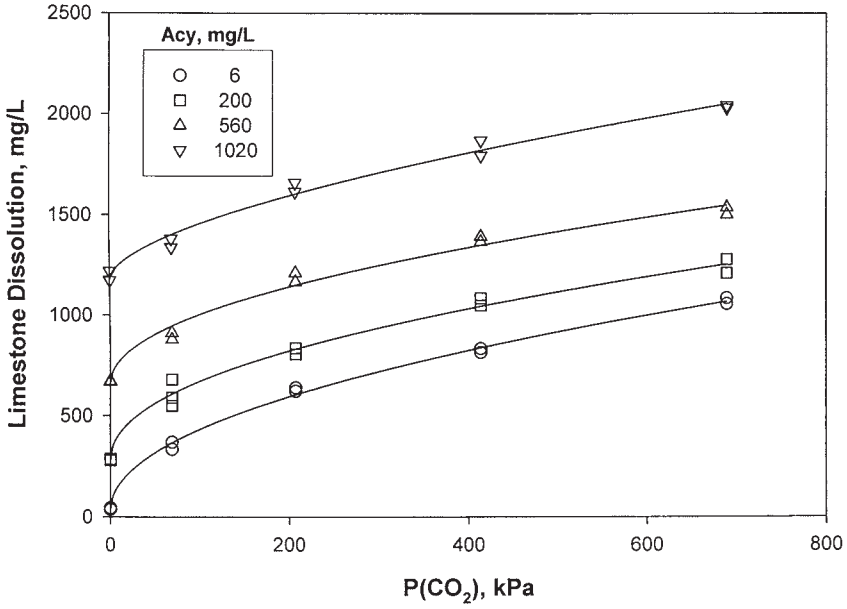

Figure 2. Effect of carbon dioxide pressure (P_{CO_2}) on limestone dissolution (LD) at each of four inlet acidities (Acy).

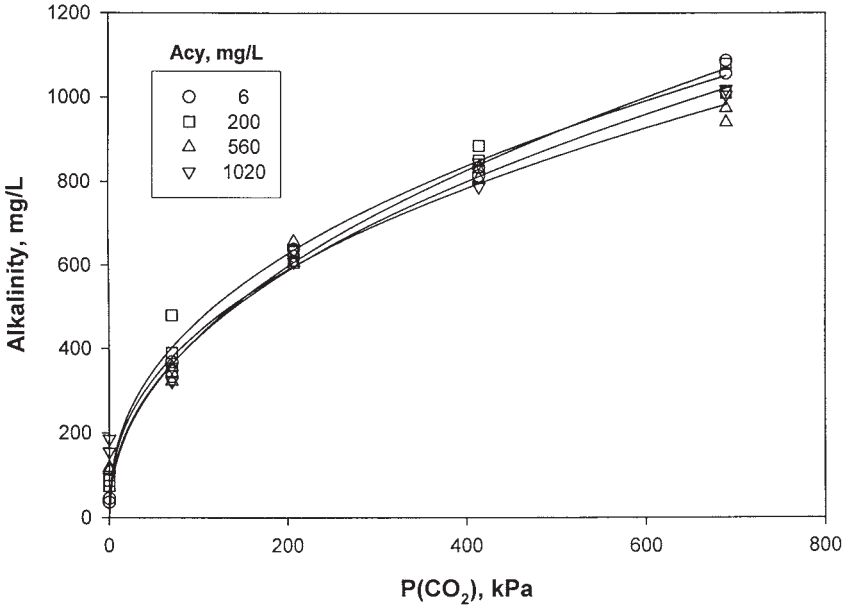

Figure 3. Effect of carbon dioxide pressure (P_{CO_2}) on effluent alkalinity (Alk) at each of four inlet acidities (Acy).

$$\text{Alk} = 58 + 38.4 \cdot (P_{CO_2}{}^{0.5}) + 0.080 \cdot (\text{Acy}) - 0.0059 \cdot (P_{CO_2}{}^{0.5}) \cdot (\text{Acy}) \quad (13)$$

$$R^2 = 0.987;\ p < 0.0001;\ df = 37;\ F = 926.50$$

High levels of dissolved carbon dioxide in the reactors' effluent depressed pH well below that predicted for air-saturated waters within the range of alkalinity concentrations observed. Effluent pH decreased with increasing acidity, averaging 6.1 (SD, 0.90), 5.8 (SD, 0.22), 5.7 (SD, 0.16), and 5.6 (SD, 0.12) for acidity treatments of 6.4, 200.5, 557.8, and 1,019.5 mg/L. Air stripping of effluent samples for 7 min increased pH to a mean (N = 36) of 7.99 (SD, 0.20). Figure 4 compares the limestone dissolution established with cycle durations of 8 and 4 min at each of two mean acidities [7.4 mg/L (SD, 2.98); 1,019.5 mg/L (SD, 7.59)] and three pressures (0, 210, 690 kPa). Inlet water temperature was 9.5°C. Local barometric pressure averaged 756 mmHg (SD, 1.3). Average settled bed heights maintained during 8-min cycle tests (60.8 cm, SD, 1.34) were not different ($p > 0.05$) than those maintained during corresponding 4-min cycle tests (60.1, SD, 2.31). Test variables Acy and P_{CO_2} affected both limestone dissolution ($F = 55.29$, $df = 2$ and 18; $p < 0.0001$) and effluent alkalinity ($F = 58.54$, $df = 2$ and 18, $p < 0.0001$). Cycle duration did not affect the influence of P_{CO_2} on limestone dissolution or effluent alkalinity at high acidity ($p > 0.05$) but did at low acidity ($p < 0.05$). In all 4- and 8-min cycle runs, limestone dissolution was described well ($R^2 > 0.99$; $p < 0.001$) by the model form $\text{LD} = a_1 + b_1 (P_{CO_2})^{0.5}$ where a_1 and b_1 are regression coefficients.

Effects of bed height on limestone dissolution and effluent alkalinity (SD, 10.14) are shown in Fig. 5 for the bed height range 27.3–77.5 cm. Duration of the test period was 64.9 h. Influent acidity averaged 365.6 mg/L (SD, 10.1) at 9.2°C corresponding to an inlet pH of 2.38. Barometric pressure averaged 734 mmHg (SD, 3.6). Effluent pH (sample not air stripped) ranged from 5.27–5.59. Observed increases in limestone dissolution and effluent alkalinity with bed height were statistically significant:

$$\text{LD} = 948 \cdot (1 - e^{-0.0534 \cdot H}) \quad (14)$$

$$R^2 = 0.929;\ p < 0.001;\ df = 69;\ F = 906.74$$

$$\text{Alk} = 622 \cdot (1 - e^{-0.0342 \cdot H}) \quad (15)$$

$$R^2 = 0.881;\ p < 0.001;\ df = 69;\ F = 510.77$$

Carbon dioxide flow rate $Q(CO_2)$ and corresponding treatment cycle in-line pH are given in Fig. 6 for each of four test pressures. Here, water temperature was 9.5°C, inlet acidity averaged 348.6 mg/L (SD, 12.26), and settled bed height averaged 56.5 cm. Inlet pH and local barometric pressure ranged between 2.36–2.38, and 723–736 mmHg, respectively. Carbon dioxide input increased with P_{CO_2} as described by the equation:

$$Q(\text{avg})_{CO_2} = 0.858 \cdot (P_{CO_2})^{0.620} \quad (16)$$

$$R^2 = 0.995;\ p < 0.0001;\ df = 11;\ F = 2034.32$$

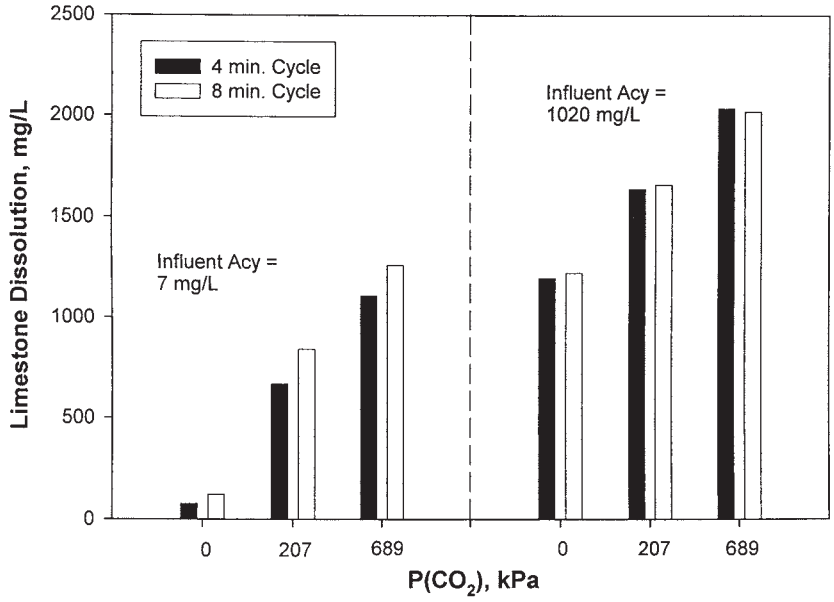

Figure 4. Effect of cycle duration (4 or 8 min) on limestone dissolution (LD) at each of three carbon dioxide operating pressures (P_{CO_2}) and two inlet acidities (Acy).

Here, $Q(avg)_{CO_2}$ is average time-based flow rate of CO_2 (L/min gas at STP) required during the 4-min treatment phase of the process. Specific (mean) values of $Q(avg)_{CO_2}$ were 2.2 L/min (SD, 0.1) at 5 kPa, 11.0 L/min (SD, 0.1) at 70 kPa, 19.0 L/min (SD, 0.2) at 140 kPa, and 27.5 L/min (SD, 0.3) at 280 kPa. Corresponding effluent alkalinity concentrations were, respectively, 172 mg/L, 320 mg/L, 453 mg/L and 631 mg/L. Increasing $Q(avg)_{CO_2}$ with P_{CO_2} amplified pH swings observed by the in-line pH probe (Fig. 6). The pH in the reactor effluent (sample not air stripped) ranged between 5.46–5.63.

Test series II—field trials

The PLB prototype produced n*et al*kaline water regardless of AMD source or operating condition. Table 1 gives water chemistry when treating AMD from Portal A at each of three test pressures. Influent temperature,

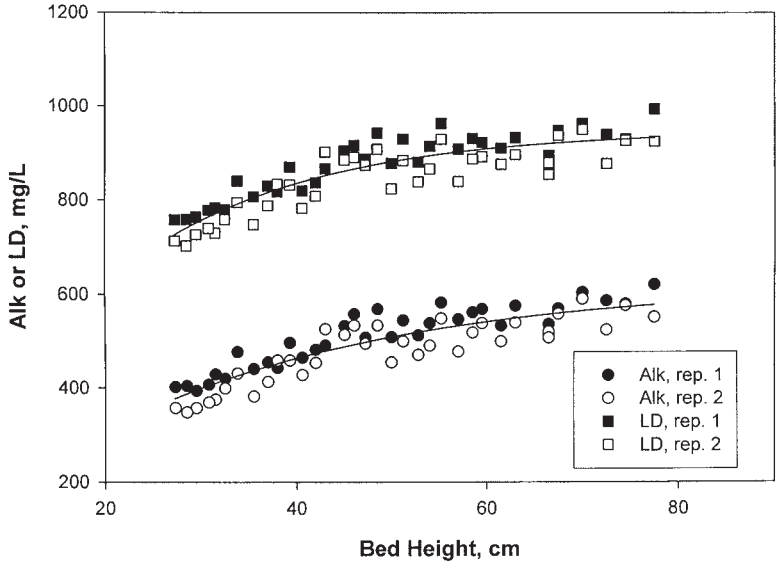

Figure 5. Effect of bed height (settled) on limestone dissolution (LD) and effluent alkalinity (Alk).

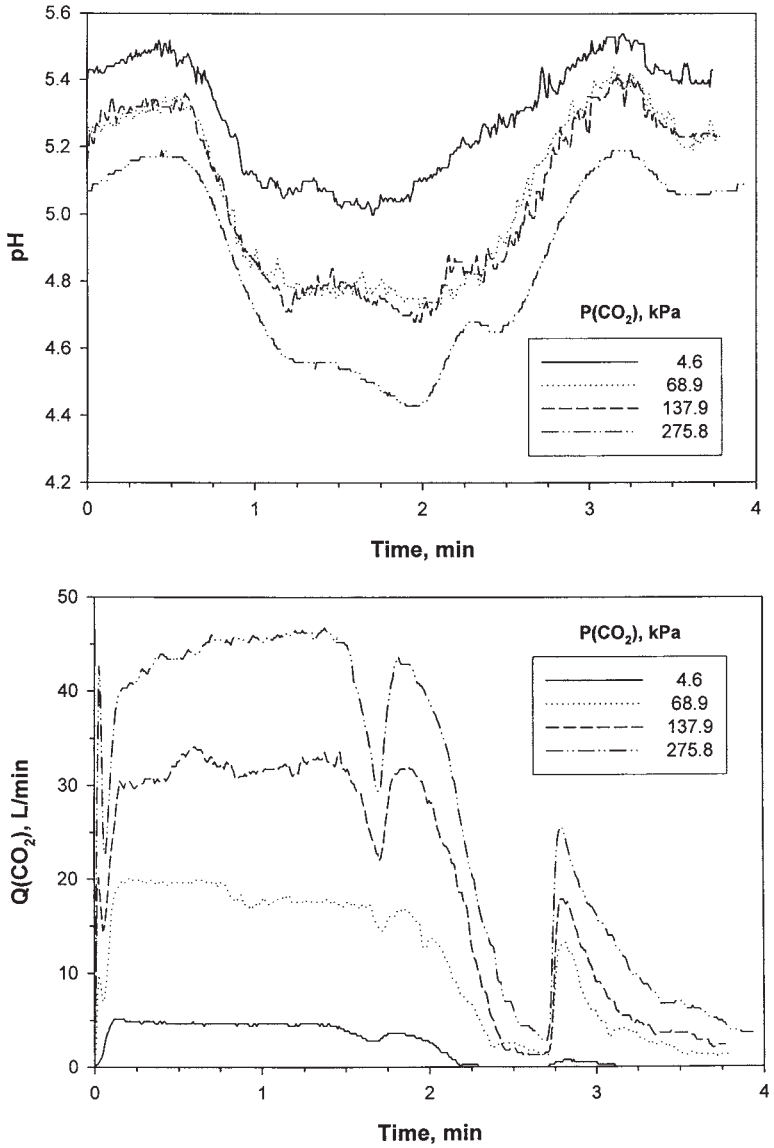

Figure 6. Changes in carbon dioxide flow rate $Q(CO_2)$ (L/min gas at STP) and treatment cycle pH during a 4-min treatment cycle at each of four operating pressures (P_{CO_2}).

dissolved oxygen, and CO_2 tension ranges were, respectively: 8.5–8.6°C; 8.0–8.3 mg/L, and 7.9–11.4 mmHg. Local barometric pressure was 716–722 mmHg. Bed height (settled) ranged between 57.8–62.2 cm. AMD inflow averaged 8.7 L/min (SD, 0.61) with the recirculating flow fixed at 9.5 L/min. Metal removal efficiencies, established by comparison of influent with effluent (filtered) concentrations, were independent of P_{CO_2} ($p > 0.05$) averaging 98.1% (SD, 0.72) for Al^{3+}, 64.5% (SD, 20.83) for Fe^{2+}, 86.8% (SD, 3.41) for Fe_T, and 5.9% (SD, 3.30) for Mn^{2+}. Increases in alkalinity with P_{CO_2} were statistically significant ($p < 0.05$). Differences between nonfiltered alkalinities and filtered sample alkalinities (Table 1) were statistically significant ($p < 0.05$) but were not related to P_{CO_2} ($p > 0.05$).

Table 2 gives influent and effluent chemistry when treating AMD from Portal A and Kyler Run without input of CO_2. Here, influent temperature, dissolved oxygen, and CO_2 tension ranges were, respectively: 8.5–8.8°C, 10.5–10.8°C; 7.4–10.0 mg/L, 4.8–6.4 mg/L; 14.6–19.0 mmHg, 16.5–20.4 mmHg. Local barometric pressure was 718–732 mmHg. Bed height (settled) ranged between 62.2–65.8 cm. AMD inflow was kept between 9.0–9.5 L/min. with the recirculating flow fixed at 9.5 L/min. Effluent pH and alkalinity were similar and acceptable, in both cases, despite differences in influent chem-

Table 1. Effect of operating pressure on changes in water chemistry across test system.

		Pressure					
		69.0 kPa		*137.9 kPa*		*193.1 kPa*	
Variable	*Infl.*	*Effl. NF*	*Effl. F*	*Effl. NF*	*Effl. F*	*Effl. NF*	*Effl. F*
pH	3.1 (0.0)	6.9 (0.1)	7.0 (0.1)	7.1 (0.0)	7.2 (0.1)	7.6 (0.1)	7.7 (0.1)
Acidity, mg/L	239 (8.2)	0	0	0	0	0	0
Alkalinity, mg/L	0	192 (33)	190 (6)	274 (0)	259 (4)	334 (17)	325 (10)
Al^{3+}, mg/L	13.4 (6.9)	13.5 (0.8)	0.5 (0.1)	13.4 (2.8)	—[a]	12.6 (1.2)	0.2 (0.0)
Fe^{2+}, mg/L	4.9 (0.3)	2.9 (0.6)	2.6 (0.4)	2.0 (0.0)	1.5 (0.1)	1.7 (0.7)	0.8 (0.6)
Fe_T mg/L	17.6 (1.6)	17.0 (0.7)	3.2 (0.3)	15.3 (1.3)	2.3 (0.0)	15.7 (1.8)	1.6 (0.1)
Mn^{2+}, mg/L	7.4 (0.3)	7.5 (0.1)	7.2 (0.2)	6.9 (0.2)	6.7 (0.0)	7.0 (0.0)	6.9 (0.3)
Ca^{2+}, mg/L	85 (5)	246 (1)	237 (10)	237 (6)	217 (6)	268 (30)	265 (15)

Infl. = influent mean, $N = 6$; Effl. NF = effluent (not filtered) mean, $N = 2$; Effl. F = effluent (filtered) mean, $N = 2$. Mean values are given in the table followed by the standard deviation in parentheses.

[a]Data not recorded.

istry. Calculated Fe^{2+} and Mn^{2+} removal efficiencies were low averaging, respectively, 22.3% and 11.2% for Portal A and 16.8% and 1.7% for Kyler Run. Calculated removal efficiencies for Al^{3+} were high, in all tests, ranging between 93.0–99.1%. Differences between nonfiltered alkalinity and filtered alkalinity averaged just 2.6% (2.0 mg/L, SD, 1.27) and were not statistically significant ($p > 0.05$). Portal A alkalinity concentrations were correlated with P_{CO_2} over the P_{CO_2} range 0–190 kPa (Tables 1 and 2):

$$\text{Alk} = 73 + 17.5 \cdot (P_{CO_2}{}^{0.5}) \qquad (17)$$
$$R^2 = 0.972;\ p < 0.001;\ df = 7;\ F = 247.32$$

DISCUSSION

Limestone dissolution

Our tests demonstrated the ability of the PLB process to neutralize acidity over the acidity range common in coal mine AMD while operating with hydraulic retention times (HRT) that represent just a fraction of that required for alternative reactor types. For example, Hedin *et al.* (1994) reported on the performance of two buried fixed beds of crushed limestone (anoxic limestone drains) operating in the plug flow reactor mode. AMD retention times ranged between 16–192 h. Corresponding acidity removals and effluent alkalinity concentrations were between 22.6–77.1% and 161—271 mg/L, respectively. Other researchers found that cone shaped or staged vertical fluidized beds of limestone required HRTs of 1.9–15 h to reduce AMD acidity 86–98% while providing effluent alkalinity concentrations of 50–150 mg/L (Maree and du Plessis, 1994). Conversely, the PLB tested here used an HRT of just 4.2–5.0 min while providing complete removal of acidity and effluent alkalinity concentrations of up to 1,080 mg/L (Fig. 3; Tables 1–2). The decrease in HRT achieved provides for reductions in capital costs related to reactor volume. Additionally,

Table 2. Effect of water source on changes in water chemistry across test system.

	Portal A			*Kyler run*		
Variable	*Infl.*	*Effl. NF*	*Effl. F*	*Infl.*	*Effl. NF*	*Effl. F*
pH	3.1 (0.0)	6.6 (0.1)	6.6 (0.0)	3.8 (0.1)	6.5 (0.1)	6.5 (0.1)
Acidity, mg/L	218 (11)	0	0	134 (4)	0	0
Alkalinity, mg/L	0	80 (2)	80 (2)	0	80 (11)	77 (12)
Al^{3+}, mg/L	14.2 (0.1)	6.6 (2.2)	0.4 (0.3)	8.5 (0.5)	2.7 (2.2)	0.4 (0.2)
Fe^{2+}, mg/L	2.9 (0.7)	2.8 (0.3)	2.1 (0.2)	10.7 (0.2)	8.7 (1.4)	8.9 (1.5)
Fe_T, mg/L	15.3 (0.6)	10.0 (1.2)	2.3 (0.5)	10.7 (1.1)	9.8 (0.6)	9.3 (1.6)
Mn^{2+}, mg/L	7.2 (0.1)	6.4 (0.2)	6.4 (0.1)	8.0 (0.4)	7.9 (0.4)	7.8 (0.4)
Ca^{2+}, mg/L	84 (3)	169 (12)	161 (3)	82 (2)	144 (2)	139 (2)

(Infl. = influent mean, $N = 3$; Effl. NF = effluent (not filtered) mean, $N = 3$; Effl. F = effluent (filtered) mean, $N = 3$). Mean values are given in the table followed by the standard deviation in parentheses.

achievement of alkalinity concentrations well above the EPA criteria of 20 mg/L allows for sidestream treatment, with blending, to further reduce reactor volume for a given process flow. In this case, gravity separation of solid reaction products [Equations (3)–(5)] would be required downstream of the treated and untreated flow mixing point. Sibrell *et al*. (2000) report a successful fivefold dilution of AMD entering the Toby Creek Treatment Plant, Pennsylvania Department of Environmental Protection, when operating a pilot-scale PLB system at a carbonator pressure (gage) of just 82 kPa. In this case, the effective flow treated was increased from 227 to 1,136 L/min.

We attribute the PLB's relatively low required hydraulic residence time and high effluent alkalinity concentrations to (1) use of limestone particles with high specific surface area, (2) hydrodynamic conditions that favor removal of oxyhydroxide reaction products while providing high levels of turbulence, and (3) maintenance of dissolved carbon dioxide concentrations well above air saturation concentrations. Regarding the latter, PLB equipment is designed to promote equilibrium between elevated gas phase partial pressures (P_i^G) of CO_2, within the carbonator, and dissolved gas tensions (P_i^L). At equilibrium $P_i^G = P_i^L$, and for all gases i present:

$$\sum_i^n P_i^G + P_{H_2O} = \sum_i^n P_i^L + P_{H_2O} \qquad (18)$$

where P_{H_2O} is water vapor pressure. From Dalton's Law, the sum on the left of Equation (18) defines total gas pressure, whereas the sum on the right defines total dissolved gas pressure. Positive gage pressures develop within the carbonator when total dissolved gas pressure minus barometric pressure is greater than zero (Watten *et al*., 1997). The P_i^L of a selected gas is directly related to the corresponding dissolved gas concentration (C_i, mg/L), and can be calculated given temperature, salinity, and appropriate Bunsen solubility coefficients (β_i), that is, from Henry's Law (Colt, 1984):

$$P_i^L = C_i \cdot \left(\frac{A}{\beta}\right) \qquad (19)$$

P_i^L is in units of mm Hg, A_i is the ratio 760/(1000 K_i), K_i is the ratio of molecular weight to molecular volume and β_i is in units of L gas/ (L · atm). C_i values are related to AMD source concentrations, transformations that occur within the reactors [Equations (1)–(9)], and CO_2 feed requirements. The latter, in agreement with gas transfer theory (Lewis and Whitman, 1924), decrease during the treatment cycle (Fig. 6) as recirculated AMD approaches the equality defined by Equation (18). The addition here of CO_2 acts to elevate limestone solubility within the reactors (Stumm and Morgan, 1996), and therefore increases potential equilibrium concentrations of effluent alkalinity. Figure 7 gives the theoretical solubility of limestone vs. P_{CO_2} calculated with the aid of geochemical modeling software (Parkhurst, 1995). Results are compared with experimental data from Lovell (1973) as well as effluent alkalinity concentrations measured during our tests [Equation (13), (15), and (17)]. All data show

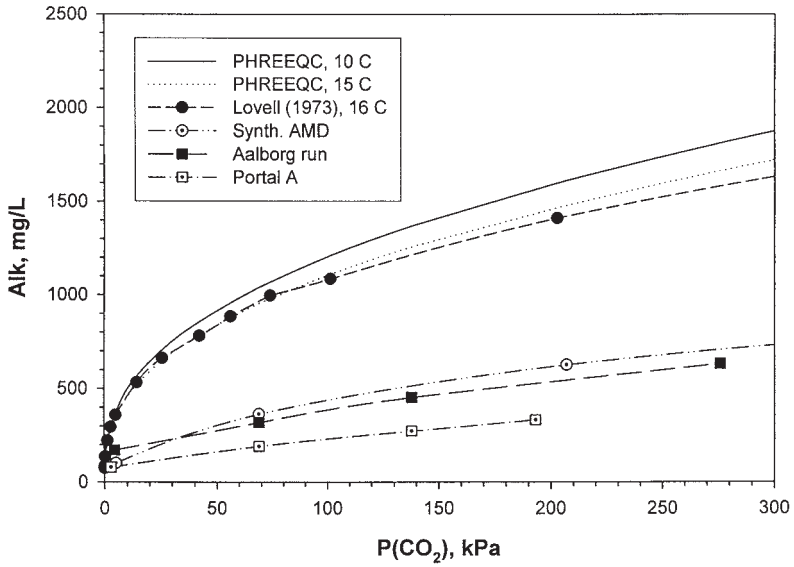

Figure 7. Effluent alkalinity (Alk) and predicted equilibrium concentrations of alkalinity vs. carbon dioxide pressure (P_{CO_2}). Synthetic AMD and Aalborg data sets refer to Test Series I runs conducted at acidities of 6.4 to 1019.5 and 350 mg/L, respectively. Portal A data refers to Test Series II runs conducted at the Toby Creek Mine Drainage Treatment Plant, Dagus Mines, PA.

a similar dependence on P_{CO_2}, although PLB data are well below calculated equilibrium concentrations. A greater degree of saturation could be achieved through an increase in settled bed height [Fig. 5, Equation (15)] or HRT. Lee (2003) evaluated the effect of HRT on PLB performance at temperatures of 12, 17, and 22°C. Here, effluent alkalinity increased linearly with HRT, for example, from 300 mg/L at HRT = 6 min to 500 mg/L at 15 min (T = 12°C; P_{CO_2} = 34.4 kPa). Temperature effects on effluent alkalinity were minor—with a carbonator pressure of 209 kPa, effluent alkalinity decreased from 900 mg/L at 12°C to 800 mg/L at 22°C (HRT = 15 min).

CO_2 addition increases limestone dissolution rates, as well as saturation concentrations, by forcing the reaction of $CaCO_3$ with CO_2 [Equation (8)], and by increasing temporarily the acidity of the AMD during treatment [Equation (7)]. The latter response, indicated by reductions in pH with increasing P_{CO_2} (Fig. 6), acts to accelerate the reaction of $CaCO_3$ with H^+ [Equation (6)]. The total forward dissolution rate is the sum of these two reactions plus the reaction of $CaCO_3$ with water [Equation (9)]. The overall response of effluent alkalinity is a square root dependence on P_{CO_2} (Fig. 3), which is similar to that predicted by the carbonate equilibrium expressions when coupled with mass and charge balances (Evangelou, 1995). Figure 8 shows the effect of P_{CO_2} on the relative contribution of each reaction component over the pH range 2.5–6.5. The dissolution rates shown were calculated based on rate constants determined experimentally for water at 10°C (Plummer *et al*., 1978). The reaction of H^+ with $CaCO_3$ decreases linearly with increasing pH, but remains the primary mechanism of limestone dissolution up to a pH of about 4.7. At pH 4.8 and above, in this example, the reaction with carbonic acid becomes dominant as P_{CO_2} is shifted from 7 to 70 kPa. This response provides a maximum fourfold increase in the overall dissolution rate above that calculated for the baseline P_{CO_2} of 7 kPa. If P_{CO_2} were shifted further to 700 kPa, the overall dissolution rate would be increased by a factor of 30. These example calculations do not include the positive effect of increasing P_{CO_2} on dissolution rate that results from linked reductions in pH, or pH buffering. In our tests (Fig. 6), measured pH was held below pH 5.5 during treatment (P_{CO_2} = 4.6–275.8 kPa), despite the development of high concentrations of bicarbonate alkalinity. The effects of dissolved carbon dioxide on equilibrium pH can be estimated based on application of the Henderson-Hasselbach equation:

$$\mathrm{pH} = \mathrm{pK_1} - \log\left(\frac{[CO_2]}{[HCO_3^-]}\right) \qquad (20)$$

where pK_1 is the negative logarithm of the equilibrium constant for the protolysis of H_2CO_3, $[CO_2]$ is dissolved carbon dioxide in mol/L and $[HCO_3^-]$ is bicarbonate in mol/L. For example, with $[HCO_3^-]$ fixed at 3 mmol/L (alkalinity = 150 mg/L), an increase in P_{CO_2} from a standard air condition (P_{CO_2} = 0.032 kPa) to tensions of 125 and 250 kPa reduces equilibrium pH from 8.7 to 5.1 and

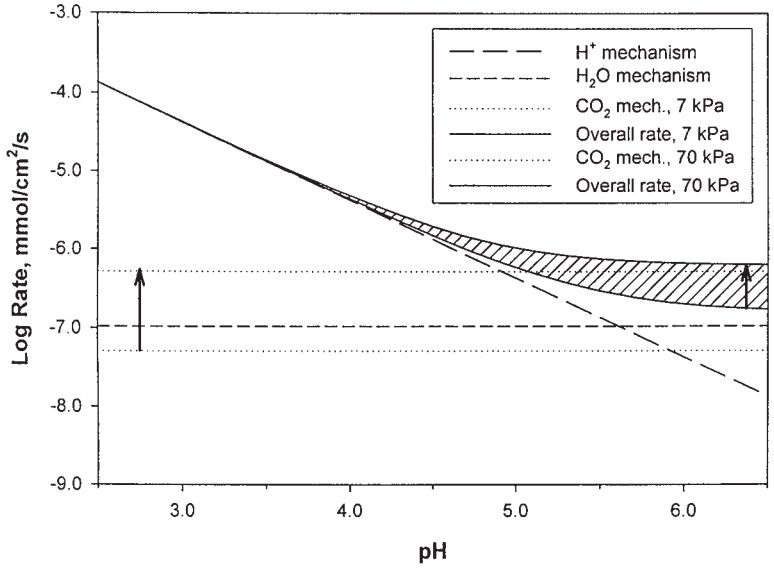

Figure 8. Effect of pH and carbon dioxide pressure on $CaCO_3$ dissolution rate kinetics. Right arrow shows a fourfold increase in the overall dissolution rate with a change in carbon dioxide pressure from 7 to 70 kPa. Left arrow shows this same pressure change increases the carbon dioxide dissolution rate mechanism [Equation (8)] 10-fold.

4.8, respectively. Values of pK_1 decrease as temperature increases (Lowenthal and Marais, 1976), causing a similar shift in pH. The pH values shown in Fig. 6 at the end of the treatment cycle (5.08–5.42) are lower than pH values measured in the effluent (5.46–5.63) given the spontaneous loss of CO_2 from solution that occurs following pressure let down at the start of the rinse/loading phase.

Figure 9 gives the overall limestone dissolution rates corresponding to data presented in Fig. 2. Rates here were based on a limestone surface area of 150 cm^2/g calculated given our particle size distribution and a shape factor of 1.75 (Geiger and Poirier, 1973). The dissolution rates shown, in general, varied between 10^{-6}–10^{-8} $mmol/cm^2/s$, which lie within the range reported for calcite, CO_2, and H_2SO_4 within stirred reaction flasks (Plummer *et al*., 1978), and bench-scale fluidized beds (Chou *et al*., 1989). Although acidity had little effect on effluent alkalinity at a given P_{CO_2} (Fig. 3), total dissolution rates rose with acidity given associated increases in $[H^+]$ [Equation (6)]. Elevation of acidity beyond the range tested can, however, retard limestone dissolution in those cases where Ca^{2+} combines with SO_4^{2-} to form gypsum at a rate that forces precipitation and scale formation on limestone surfaces. The solubility product of gypsum governs this response as well as hydrodynamic conditions within the reactor. Sulfate concentrations above 10 mmol/L have caused gypsum formation and complete inhibition of limestone dissolution within stirred reaction flasks (Sverdrup and Bjerle, 1982). This condition corresponds to a pH limit (low) of 2.0 in dilute H_2SO_4. Limestone dissolution has continued without inhibition when treating acidities as high as 5,000 mg/L in both fluidized bed (Ghem, 1944) and PLB reactors (Sibrell *et al*., 2000). In the latter case, the pH of the AMD treated was 1.6, with a corresponding sulfate concentration of 50 mmol/L. Increasing base metal content will also occur with an increase in acidity or SO_4^{2-}. This correlation, in turn, promotes alternative scale forming reactions, particularly those associated with Fe^{3+} and Al^{3+}. Fe^{3+} and Al^{3+} undergo hydrolysis reactions [Equation (3) and (4)] forming precipitates that quickly coat limestone surfaces and plug void space within packed bed reactors (Hedin *et al*., 1994). Consequently, limestone use has not been recommended for sites with acidity >50 mg/L or $Fe_T > 5$ mg/L (Skousen *et al*., 1995). Iron-based armoring has been avoided, when iron is present as Fe^{2+}, by establishing anoxic conditions within the reactor. This prevents oxidation of Fe^{2+} to Fe^{3+} and its subsequent hydrolysis to hydrous ferric oxide $[Fe(OH)_3]$. Deoxygenation is achieved, when required, in a pretreatment step based on microbial oxidation of organic matter such as spent mushroom compost (Hedin *et al*., 1994). Deoxygenation will not prevent Al^{3+}-based scale formation, and so application of this approach is limited unless the scale is periodically flushed from the bed.

Field trials

The PLB process was designed to circumvent iron and aluminum based armoring by increasing limestone dis-

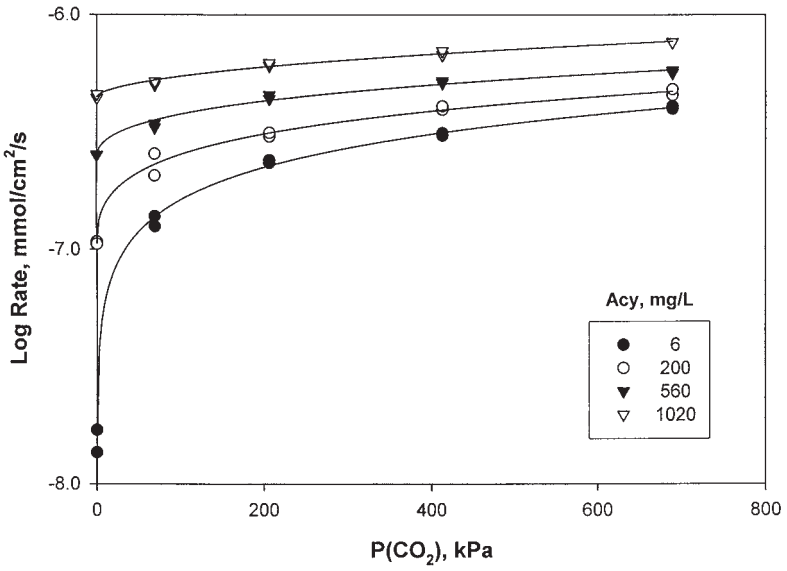

Figure 9. Effect of carbon dioxide pressure (P_{CO_2}) on limestone dissolution rate ($mmol/cm^2/s$) calculated for each of four test acidities (Acy, mg/L as $CaCO_3$).

solution with elevated dissolved carbon dioxide, and by creating hydrodynamic conditions that keep particle surfaces/bed voids clean of hydrolysis reaction products. Table 1 data show effective AMD treatment during short-term runs at the Toby Creek test site. Effluent alkalinity was high and easily controlled by altering P_{CO2}. Longer term tests at the same site with a pilot scale (227L/min.) PLB reactor (Sibrell *et al*., 2000) demonstrated similar levels of treatment could be achieved, without armoring, despite acidity and Fe_T concentrations that exceeded recommended limits by factors of 5.2 and 4.2, respectively (Skousen, 1998). Here, 10,000 m^3 of AMD was treated during a 30-day period with effluent alkalinity concentrations of 50 to 300 mg/L, depending on carbonator operating pressures (0–117 kPa). More recently, Sibrell *et al.* (2003) evaluated the pilot scale PLB reactor at a second site (Friendship Hill National Historic Site, Point Marion, PA) that provided AMD with unusually high concentrations of acidity (1,000 mg/L), Fe_T (200 mg/L) and Al^{3+} (60 mg/L). Armoring occurs here rapidly when using conventional fluidized bed reactors (Hammarstrom *et al*., 2003), that is, within 48 h limestone grains developed a rind of gypsum encapsulated by a 10–30 μm-thick Fe–Al hydroxysulfate coating, causing a drop in effluent pH from 7 to less than 4. Despite the high potential for armoring, the PLB reactor continued to provide a high limestone utilization efficiency during a 14-month test period. About 50,000 m^3 of AMD was successfully treated with the mine drainage pH increasing from 2.5 to a mean of 6.8. Limestone consumption and metal hydroxide sludge production (3–5% solids content) totaled 50,000 and 450,000 kg, respectively. Metal removal was related to the ability of the PLB process, and limestone based-processes in general, to raise the AMD pH above that required for hydrolysis and precipitation of Fe^{3+} and Al^{3+} (about pH 5), but not Fe^{2+} and Mn^{2+} (pH $>$ 9). This limitation is evident in the Toby Creek and Kyler Run data (Tables 1 and 2)—Fe^{3+} and Al^{3+} removals were high and Fe^{2+} and Mn^{2+} removals were low. A trend towards higher removal of Fe^{2+} with increasing P_{CO2} was observed at Toby Creek (Table 1), which may indicate the formation of siderite ($FeCO_3$) (Hedin *et al*., 1994). This relationship was not, however, statistically significant ($p > 0.05$). Siderite solids in sludge are undesirable given the potential for contributing acidity during conversion to $Fe(OH)_3$. Likewise, there is potential for formation of rhodochrosite ($MnCO_3$), also capable of contributing acidity, but this reaction path is favored by elevated pH and does not appear to be important given our mean Mn^{2+} removal efficiency of just 4.1% (Tables 1 and 2). The concentration of Mn^{2+}, Fe_T, and the ratio of Fe^{2+}/Fe^{3+} will vary with the AMD source. When required, complete removal of Fe^{2+} and Mn^{2+} with PLB or other oxic limestone reactor types will require a pre- or posttreatment oxidation step based on use of reagents or biochemical reactors such as the Fe^{2+} oxidizing trickling filter (Lovell, 1973) and the Mn^{2+} oxidizing horizontal bed (Rose *et al*., 2003). In posttreatment oxidation applications, the effluent alkalinity must be sufficiently high to neutralize the acidity generated during oxidation/hydrolysis reactions. In pretreatment oxidation applications, the acidity generated is neutralized by limestone within the PLB reactors and will, therefore, reduce the CO_2 feed rate required for target system operating pressures.

Predicting performance

Application of the PLB process will be determined in part by its comparative economics; variable costs of operation include limestone and carbon dioxide consumption rates that, in turn, are related to operating conditions such as inlet acidity and target effluent alkalinity concentrations. The effects of acidity and operating pressure on CO_2 feed requirements can be predicted based on Equations (18) and (19), and by performing a material balance on dissolved carbon dioxide, for example, dissolved carbon dioxide in the reactors' effluent $[CO_2]_{Effluent}$, is related to the AMD source concentration $[CO_2]_{AMD}$, the carbonator gas feed rate (M_{CO_2}/L), and the net increase in dissolved carbon dioxide that occurs following acidity neutralization and effluent alkalinity production [0.44 · (Acy − Alk)]:

$$[CO_2]_{Effluent} = [CO_2]_{AMD} + (M_{CO_2}/L) + 0.44 \cdot (Acy - Alk) \quad (21)$$

Effluent alkalinity, in turn, has been described by the model form $Alk = a_1 + b_1(P_{CO_2})^{0.5}$ [Equation (17)], where a_1 and b_1 are regression coefficients developed for a specific AMD source. Combining this model with Equations (18), (19), and (21) allows calculation of required carbonator gas feed rates for a target effluent alkalinity:

$$\frac{M_{CO_2}}{L} = 7.52 \cdot \left(\frac{\beta}{A}\right)_{CO_2} \cdot \left(\frac{Alk - a_1}{b_1}\right)^2 - (0.44 \cdot (Acy - Alk) + [CO_2]_{AMD}) \quad (22)$$

where 7.52 converts kPa to units of mmHg. The ratio M_{CO_2}/L can be reduced, or in some cases eliminated, through transfer of CO_2 from system effluent to system influent (Watten, 1999). The gas recycle rate (R_{crit}), providing a target effluent alkalinity without a gas feed to the carbonator is obtained from a similar material balance:

$$R_{crit} = 1 - \left\{ \frac{0.44 \cdot (Acy - Alk) + [CO_2]_{AMD}}{7.52 \cdot \left(\frac{\beta}{A}\right)_{CO_2} \cdot \left(\frac{Alk - a_1}{b_1}\right)^2} \right\} \quad (23)$$

R values represent the fraction of $[CO_2]_{Effluent}$ recycled, and so values must vary from 0 to 1. If the calculated R_{crit} exceeds 1.0, or the selected R is less than R_{crit}, a gas feed is required. In this case:

$$\frac{M_{CO2}}{L} = \left\{7.52 \cdot \left(\frac{\beta}{A}\right)_{CO_2} \cdot \left(\frac{Alk - a_1}{b_1}\right)^2 \cdot (1 - R)\right\} - \{0.44 \cdot (Acy - Alk) + [CO_2]_{AMD}\} \quad (24)$$

If the selected R exceeds R_{crit}, P_{CO_2} will rise above that required to achieve the target effluent alkalinity. We can solve for the resultant steady-state effluent alkalinity given selected values for R, Acy, $[CO_2]_{AMD}$, and M_{CO_2}/L through application of Equation (24) and the quadratic equation, that is,

$$Alk = \frac{-b_2 \pm \sqrt{b_2^2 - 4a_2c_2}}{2a_2} \quad (25)$$

where in our case the coefficients of the equation are:

$$a_2 = \frac{1}{b_1^2} \cdot 7.52 \cdot \left(\frac{\beta}{A}\right)_{CO_2} \cdot (1 - R) \quad (26)$$

$$b_2 = 0.44 - 2 \cdot \frac{a_1}{b_1^2} \cdot 7.52 \cdot \left(\frac{\beta}{A}\right)_{CO_2} \cdot (1 - R) \quad (27)$$

$$c_2 = \left[\frac{a_1^2}{b_1^2} \cdot 7.52 \cdot \left(\frac{\beta}{A}\right)_{CO_2} \cdot (1 - R)\right] - 0.44 \cdot Acy - \frac{M_{CO_2}}{L} - [CO_2]_{AMD} \quad (28)$$

Figure 10 shows the positive effect of increases in R and Acy on effluent alkalinity as predicted by Equation (25). In this example, a rise in Acy from 100 to 1,500 mg/L increased effluent alkalinity from 99 to 266 mg/L. Effluent alkalinity was elevated further to a high of 710 mg/L as R approached 0.95. Effluent alkalinity will exceed the values shown when (M_{CO_2}/L) and $[CO_2]_{AMD}$ are set above the baseline values of 0.0 used in the example calculations. A $[CO_2]_{AMD}$ well above the air saturation concentration is common in AMD (Pearson *et al*., 1982; Jageman *et al*., 1988; Hedin *et al*., 1994), and represents, with application of the PLB process, an asset that should be conserved prior to treatment. For example, Jageman *et al*. (1988) give carbonate concentrations for waters released from three coal mines prior to treatment with hydrated lime. At 10°C and a barometric pressure of 760 mmHg, the reported carbonates equate to $[CO_2]_{AMD}$ concentrations of about 200, 290, and 340 mg/L. The corresponding air saturation concentration of dissolved carbon dioxide is just 0.75 mg/L. Using a $[CO_2]_{AMD}$ of 300 mg/L

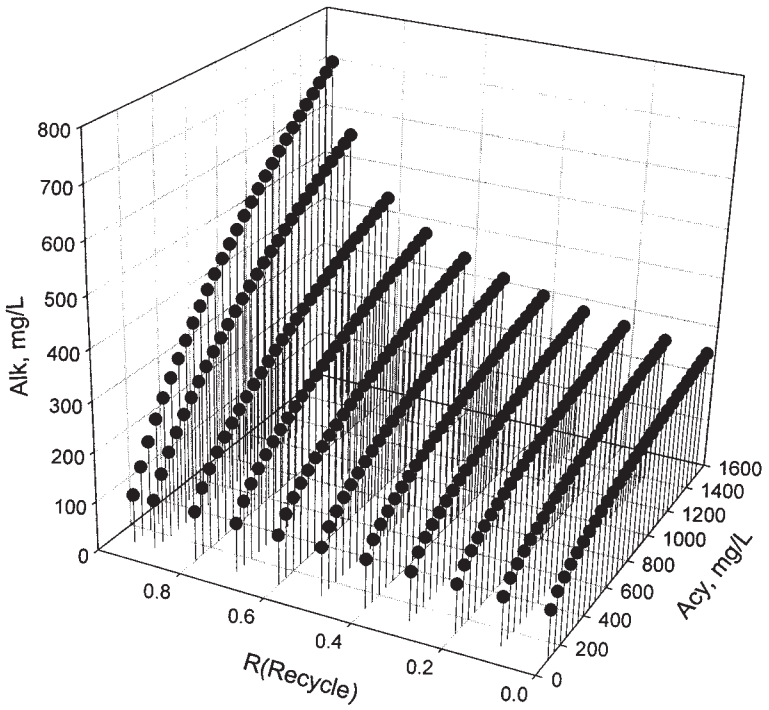

Figure 10. Effect of inlet acidity (Acy) and efficiency of carbon dioxide recovery (R) on effluent alkalinity (Alk), when Alk = 93.7 + 35.7(P_{CO_2})$^{0.5}$, T = 10°C and barometric pressure = 760 mmHg.

in Equation (25) elevates effluent alkalinity from the previous example of 100 mg/L (Acy = 100, $R = 0.95$) to 477 mg/L. Figure 3 and Table 1 show the additional increases in effluent alkalinity that can be achieved with $M_{CO_2}/L > 0$. As M_{CO_2}/L rises, however, conversion of CO_2 applied to effluent alkalinity decreases, for example, conversion efficiency calculated for runs used to establish Fig. 6 was 30.2% at $M_{CO_2}/L = 409$ mg/L, 14.2% at $M_{CO_2}/L = 2{,}088$ mg/L, 11.9% at $M_{CO_2}/L = 3{,}632$ mg/L, and 11.6% at $M_{CO_2}/L = 5{,}296$ mg/L. Therefore, recovery and reuse of dissolved carbon dioxide in reactor effluent becomes increasingly important as requirements for effluent alkalinity are elevated to satisfy target dilution ratios or seasonal changes in AMD composition. Selection of the least cost set of operating conditions, including dilution ratio, will be related to local costs of CO_2, power, reactor capital (amortized) as well as the relationship between R and CO_2 recovery costs. CO_2 recovery can be accomplished with equipment designed to provide gas–liquid interfacial area within isolated gas transfer chambers (Watten, 1999), for example, Sibrell *et al*. (2000) used a linked pair of packed towers (2 m of 3.8 cm plastic packing) for both CO_2 stripping and absorption. CO_2 rich gas generated in the stripping tower receiving PLB effluent was forced, by a blower, through an absorption tower that received untreated AMD. CO_2 lean gas exiting the absorber was redirected into the stripper to complete a closed gas recirculation loop. Gas and liquid flows in both towers were countercurrent. Use of the recovery step increased $[CO_2]_{AMD}$ about 3.7-fold to 396 mg/L and provided 102.4 kg/day of CO_2 with a calculated R of 0.24. In recent laboratory tests, we have increased R to 0.64 by raising the tower height to 6.1 m and through the use of smaller plastic packing (1.6 cm). R can be increased further through the use of sequential treatment, or staging, and by control of pressure within individual stripper and absorber components, that is, negative gage pressures will accelerate CO_2 stripping, and positive gage pressures will accelerate CO_2 absorption (Watten, 1999).

SUMMARY

The PLB prototype effectively neutralized sulfuric acid acidity, over the range 6–1033 mg/L, while concurrently providing high concentrations of effluent alkalinity despite an HRT of just 4.2–5.0 min. This trait provides potential for reductions in treatment costs related to reactor volume, and may also be of value when treating other types of acid streams such as electroplating and metal pickling wastes. Effluent alkalinity and limestone dissolution rose with increases in Acy and P_{CO_2} according to the general model $Y = a + b\,(P_{CO_2})^{0.5} + c\,(\text{Acy}) - d\,(P_{CO_2})^{0.5}\,(\text{AC})$, where a, b, c, and d are regression coefficients. With acidity fixed, limestone dissolution and effluent alkalinity increased with $(P_{CO_2})^{0.5}$ both in the laboratory and in the field. Elevation of P_{CO_2} increased gas requirements (M_{CO_2}/L) following the model $(P_{CO_2})^{0.6}$, resulting in a greater degree of pH buffering (depression) within the reactor, a rise in limestone solubility, and an increase in the limestone dissolution rate related to carbonic acid attack. Application of the performance algorithms we developed demonstrated that gas requirements for a selected P_{CO_2} are reduced as inlet acidity and dissolved carbon dioxide rise and when efficiency of the off-gas recycling increases. Our concept of conserving dissolved carbon dioxide present in the AMD, and recovering dissolved carbon dioxide present in the treatment unit effluent could provide a means of enhancing the performance of fixed-bed limestone reactors like the anoxic limestone drain. Here, gas recovery would require an energy input creating a hybrid passive/active system with greater flexibility in effluent alkalinity. Limestone dissolution and effluent alkalinity decreased, at an increasing rate, with reductions in bed height H (range 27.3–77.5 cm) as described by the general model $Y = a\,(1 - e^{bH})$ where a and b are regression coefficients. Field trials demonstrate the PLB process is capable of raising the pH of AMD above that required for hydrolysis and precipitation of Fe^{3+} and Al^{3+}, but not Fe^{2+} and Mn^{2+}. The PLB process provides an added benefit of sequestering carbon dioxide, a greenhouse gas, when the alkalinity added to AMD is less than or equal to the saturation concentration of $CaCO_3$ [Equation (8)]. The latter is fixed by temperature, salinity, and P_{CO_2}. In this application, waste gas streams containing carbon dioxide would be directed into the PLB absorption components either with or without use of a carbon dioxide enrichment/separation step.

ACKNOWLEDGMENTS

This project was funded in part by the U.S. Department of Agriculture, Agricultural Research Service (Agreement No. 59-1930-1-130), and the USGS State Partnership Program (No. 1445-CA09-0014). We thank A.E. Friedrich, Division of Mine Hazards, Pennsylvania Department of Environmental Protection, for coordinating field trials at the Toby Creek Mine Drainage Treatment Plant and D. Smith for assistance in statistical analyses.

REFERENCES

APHA (AMERICAN PUBLIC HEALTH ASSOCIATION, AMERICAN WATER WORKS ASSOCIATION AND WATER ENVIRONMENT FEDERATION]. (1995). *Standard*

Methods for the Examination of Water and Wastewater, 19th ed. Washington, D.C: APHA.

CEQ (COUNCIL on ENVIRONMENTAL QUALITY). (1981). *Environmental Trends. Executive Office of the President*. Washington, D.C: CEQ.

CHOU, L., GARRELS, R.M., and WOLLAST, R. (1989). Comparative study of the kinetics and mechanisms of dissolution of carbonate minerals. *Chem. Geol*. **78,** 269.

CLEASBY, J.H., and BAUMANN, E.R. (1977). *Backwash of Granular Filters used in Wastewater Filtration. Rep. No. 600/2-77-016*. Cincinnati, OH: U.S. EPA.

COLE, M.B., ARNOLD, D.E., and WATTEN, B.J. (2001a). Physiological and behavioral responses of stonefly nymphs to enhance limestone treatment of acid mine drainage. *Water Res*. **35,** 625.

COLE, M.B., ARNOLD, D.E., WATTEN, B.J., and KRISE, W.F. (2001b). Haematological and physiological responses of brook char to untreated and limestone-neutralized acid mine drainage. *J. Fish Biol*. **59,** 79.

COLT, J. (1984). *Computation of dissolved gas concentrations in water as functions of temperature, salinity and pressure.* Bethesda, MD: American Fisheries Society Special Publication 14.

DEMPSEY, B.A., and JEON, B. (2001). Characteristics of sludge produced from passive treatment of mine drainage. *Geochem. Explor. Environ. Anal.* **1,** 89.

EDEN, G.E., and TRUESDALE, G.A. (1950). Treatment of waste waters from the pickling of steel. *J. Iron Steel Inst.* **164,** 281.

EVANGELOU, V.P. (1995). *Pyrite Oxidation and Its Control*. Boca Raton, FL: CRC Press.

GEIGER, G.H., and POIRIER, D.R. (1973). *Transport Phenomena in Metallurgy*. Reading, MA: Addison-Wesley, p. 97.

GHEM, H.W. (1944). Neutralization of acid waste waters with an up-flow expanded limestone bed. *Sewage Wks. J.* **16,** 104.

HAMMARSTROM, J.M., SIBRELL, P.L., and BELKIN, H.E. (2003). Characterization of limestone reacted with acid-mine drainage in a pulsed limestone bed treatment system at the Friendship Hill National Historical Site, Pennsylvania, USA. *Appl. Geochem.* **18,** 1705.

HEDIN, R.J., WATZLAF, G.R., and NAIRN, R.W. (1994). Passive treatment of coal mine drainage with limestone. *J. Environ. Qual*. **23,** 1338.

INGERSOLL, C.G., MOUNT, D.R., GULLEY, D.D., La POINT, T.W., and BERGMAN, H.L. (1990). Effects of pH, aluminum, and calcium on survival and growth of eggs and fry of brook trout. *Can. J. Fish. Aqua. Sci*. **47,** 1580.

JAGEMAN, T.C., YOKLEY, R.A., and HEUNISCH, G.W. (1988). The use of pre-aeration to reduce the cost of neutralizing acid mine drainage. In *Proc. 5th Annual Meeting, American Society for Surface Mining and Reclamation, Pittsburgh, Pennsylvania*, p. 131.

LEE, P.C. (2003). Comparison of two methods for estimating pesticide volatilization from turf, characterizing a pulsed limestone bed reactor to treat high acidity water, and thermal analysis model of zero water exchange indoor shrimp farming systems. Ph.D. dissertation, Cornell University, Ithaca, NY.

LEWIS, W.K., and WHITMAN, W.C. (1924). Principles of gas absorption. *J. Ind. Eng. Chem*., **16,** 1215.

LOVELL, H.L. (1973). *An Appraisal of Neutralization Processes to Treat Coal Mine Drainage. Rep. No. 670/2-73-093*. Washington, D.C: U.S. EPA.

LOWENTHAL, R.E., and MARASI, G.V. (1976). *Carbonate Chemistry of Aquatic Systems, Theory and Application*. Ann Arbor, MI: Ann Arbor Science Publications.

MAREE, J.P., and DU PLESSIS, P. (1994). Neutralization of acid mine water with calcium carbonate. *Water Sci. Technol.* **29,** 285.

MAREE, J.P., DU PLESSIS, P., and VAN DER WALT, C.J. (1992). Treatment of acid effluents with limestone instead of lime. *Water Sci. Technol.* **26,** 345.

MAREE, J.P., VAN TONDER, G.J., MILLARD, P., and ERASMUS, T.C. (1996). Pilot-scale neutralisation of underground mine water. *Water Sci. Technol.* **34,** 141.

MITCHELL, K.G., and WILDEMAN, T.R. (1996). Solubility of Fe(III) and Al in AMD by modeling and experiment. In *Proc. 13th Annual Meeting American Society for Surface Mining and Reclamation, Knoxville, Tenn.*, p. 681.

OLEM, H. (1991). *Liming Acidic Surface Waters*. Chelsea, MI: Lewis Publishers.

PARKHURST, D.L. 1995. *User's Guide to PHREEQC—A Computer Program for Speciation, Reaction-Path, Advective Transport, and Inverse Geochemical Calculation*. U.S. Geological Survey—Water Resources Investigations Report 95-4227.

PEARSON, F.H., and McDONNELL, A.J. (1975a). Use of crushed limestone to neutralize acid wastes. *J. Environ. Eng. Div*. ASCE **101,** 139.

PEARSON, F.H., and MCDONNELL, A.J. (1975b). Limestone barriers to neutralize acidic streams. *J. Environ. Eng. Div. ASCE* **101,** 425.

PEARSON, F., MCBRIDE, S., and BATCHELER, N. (1982). Decarbonation of limestone-treated mine drainage. *J. Environ. Eng. Div. ASCE* **108,** 957.

PLUMMER, L.N., WIGLEY, T.M.L., and PARKHURST, D.L. (1978). The kinetics of calcite dissolution in CO_2–water systems at 5° to 60°C and 0.0 to 1.0 ATM CO_2. *Am. J. Sci*. **278,** 179.

ROSE, A.W., SHAH, P.J., and MEANS, B. (2003). Case studies of limestone-bed passive systems for manganese removal

from acid mine drainage. In *Proc. 20th Annual Meeting American Society for Mining and Reclamation, Billings, Montana*, pp. 1059–1078.

SHERWOOD, T.K., PIGFORD, R.L., and WILKE, C.R. (1975). *Mass Transfer*. Kogakusha, Tokyo: McGraw Hill.

SIBRELL, P.L., and WATTEN, B.J. (2003). Evaluation of sludge produced by limestone neutralization of AMD at the Friendship Hill National Historic Site. In *Proc. 20th Annual Meeting American Society for Mining and Reclamation*, Billings, Montana.

SIBRELL, P.L., WATTEN, B.J., FRIEDRICH, A.E., and VINCI, B.J. (2000). ARD remediation with limestone in a CO_2 pressurized reactor. In *Proc. 5th International Conference on Acid Rock Drainage, Society for Mining, Metallurgy, and Exploration*, Denver, Colorado.

SIBRELL, P.L., WATTEN, B.J., and BOONE, T. (2003). Remediation of acid mine drainage at the Friendship Hill National Historic Site with pulsed limestone bed process. *Hydrometallurgy 2003*, Vancouver, BC, Canada, August 24–27, 2003.

SKOUSEN, J. (1998). Chemicals for treating acid mine drainage. *Green Lands* **18,** 36.

SKOUSEN, J. POLITAN, K., HILTON, T., and MEEK, A. (1995). Acid mine drainage treatment systems: Chemicals and costs. In: Skousen, J.G., Ziemkiwicz, P.F., Eds. *Acid Mine Drainage Control and Treatment*. Morgantown, WV: West Virginia University and the National Mine Land Reclamation Center, p. 121.

STARNES, L.B., and GASPER, D.C. (1995). Effects of surface mining on aquatic resources in North America. *Fisheries* **20,** 20.

STUMM, W., and MORGAN, J.J. (1996). *Aquatic Chemistry*. New York: John Wiley & Sons.

SUMMERFELT, S.T., and CLEASBY, J.L. (1993). *Hydraulics in Fluidized-Bed Biological Reactors. Techniques for Modern Aquaculture*. St. Joseph, MI: ASAE.

SVERDRUP, H., and BJERLE, I. (1982). Dissolution of calcite and other related minerals in acidic aqueous solution in a pH-stat. *Vatten* **38,** 87.

SVERDRUP, H.U. (1984). Calcite dissolution kinetics and lake neutralization. Ph.D. Thesis, Lund Institute of Technology, Lund, Sweden.

WATTEN, B.J. (1999). *Process and Apparatus for Carbon Dioxide Pretreatment and Accelerated Limestone Dissolution for Treatment of Acidified Water. U.S. Patent 5914046*. Washington, D.C: U.S. DOC.

WATTEN, B.J., BOYD, C.E., SCHWARTZ, M.F., SUMMERFELT, S.T., and BRAZIL, B.L. (2003). Feasibility of measuring carbon dioxide based on headspace partial pressures. *Aquacult. Eng.* **30,** 83.

WATTEN, B.J., SMITH, D.R., and RIDGE, W.J. (1997). Continuous monitoring of dissolved oxygen and total dissolved gas pressure based on head-space partial pressures. *J. World Aquacult. Soc.* **28,** 316.

WILMOTH, R.C. (1974). *Limestone and Limestone-Lime Neutralization of Acid Mine Drainage. Rep. No. 670/2-74-051*. Cincinnati, OH: U.S. EPA.

WHEATLAND, A.B., and BORNE, B.J. (1962). Neutralization of acidic waste waters in beds of calcined magnesite. *Water Waste Treatment* **Jan/Feb,** 560.

ZIEMKIEWICZ, P.F., SKOUSEN, J.G., BRANT, D.L., STERNER, P.L., and LOVETT, R.J. (1997). Acid mine drainage treatment with armored limestone in open limestone channels. *J. Environ. Qual.* **26,** 1017.

ZURBUCH, P.E. (1963). Dissolving limestone from revolving drums in flowing water. *Trans. Am. Fish. Soc*. **93,** 173.